SOIL-PILE-STRUCTURE INTERACTION IN LIQUEFIABLE GROUND THROUGH MULTI-DIMENSIONAL SHAKING TABLE TESTS USING E-DEFENSE FACILITY

H. Suzuki[1], K. Tokimatsu[2], M. Sato[3] and K. Tabata[4]

[1] Assistant Professor, Dept. Architecture and Building Engineering, Tokyo Institute of Technology, Japan
[2] Professor, Dept. Architecture and Building Engineering, Tokyo Institute of Technology, Japan
[3] Principal Senior Researcher, Disaster Prevention System Research Center, NIED, Japan
[4] Researcher, Hyogo Earthquake Engineering Research Center, NIED, Japan

Email: hsuzuki@arch.titech.ac.jp, kohji@o.cc.titech.ac.jp

ABSTRACT:

Geotechnical shaking table tests were conducted using the E-Defense facility to investigate the response and failure of a nearly full-scale pile-structure system in a liquefiable sand deposit subjected to multi-dimensional loading. A soil-pile-foundation system consisting of a foundation supported on a 3x3 steel pile group in a dry sand deposit was set in a cylindrical laminar box and then moved on to the shaking table for saturation of the ground, placement of a superstructure, if any, and the liquefaction tests. The sand deposit consisted of two layers including an underlying non-liquefiable dense sand layer and a liquefiable medium dense sand layer. Two types of ground motion having different predominant periods were used as input two-dimensional motions. The test results give detailed information on the distributions of bending strain and axial strain within the pile group as well as the ground response and pore water pressure generation in the soil around the piles. Not only the maximum acceleration but also the type of the input motion significantly affects the occurrence of soil liquefaction as well as soil-pile-structure interaction. All the pile heads yielded during the final test with high-level of input acceleration, causing residual deformation and settlement of the foundation. The pile damage was particularly significant on the leading side of the strong axis of the inertial force and ground displacement, suggesting that the difference in deformation mode of piles was affected by the difference in both axial strains and bending strains within the pile group.

KEYWORDS: Pile group, liquefaction, multi-dimensional shaking table tests, stresses, failure mechanism

1. INTRODUCTION

To estimate inertial and kinematic effects on pile damage, soil-pile-structure interaction has been investigated through physical model tests using 1G and centrifugal shake tables. Most of the tests, however, were conducted under one-dimensional loading (e.g. Mizuno et al., 1997, Tamura et al., 1998 and Boulanger et al., 1999) and rarely made under multi-dimensional loading conditions (e.g. Saito et al., 2002) that actually occurred in the field. It is therefore important to simulate soil-pile-structure interaction under multi-dimensional loading and to investigate inertial and kinematic effects on pile damage based on the test results.

To investigate inertial and kinematic effects on failure and deformation modes of pile group during multi-dimensional shaking, physical tests on soil-pile-structure models were conducted using the E-Defense at the Hyogo Earthquake Engineering Research Center of the National Research Institute for Earth Science and Disaster Prevention (NIED) (Tabata and Sato, 2006, and Tabata et al., 2007, Tokimatsu et al., 2007). The E-defense facility is one of the largest shaking tables in the world and could simulate three-dimensional ground motions. Two test series on soil-pile-structure systems, one with dry sand and the other with saturated sand, were conducted using a cylindrical laminar box placed on the shaking table. The objective of this study is to outline the geotechnical shaking table test procedure using the E-Defense facility and to investigate dynamic soil-pile-structure interaction involving failure mechanism of pile foundation in a liquefiable sand deposit.

2. MULTI-DIMENSIONAL SHAKING TABLE TESTS

The E-Defense shaking table platform has a dimension of 15 m long and 20 m wide. Fig. 1 and Photo 1 show a test model constructed in a cylindrical laminar box 6.5 m high with an outside diameter of 8.0 m. It consists of forty-one stacked ring flames, enabling two-dimensional shear deformation of the inside soil.

A 3x3 steel pile group was used for the test. The piles were labeled A1 to C3 according to their locations within the pile group, as shown in Fig. 1. Each pile had a diameter of 152.4 mm and a wall thickness of 2.0 mm. The piles were set up with a horizontal space of four-pile diameters center to center. Their tips were jointed to the laminar box base with pins and their heads were fixed to the foundation of a weight of 10 tons.

The sand deposit prepared in the laminar box consisted of two layers, including a liquefiable layer with a thickness of 5.4 m and an underlying non-liquefiable layer with a thickness of 0.8 m. Dry Albany sand from Australia was used for preparing the sand deposit. Fig. 2 shows the grain size distribution of the sand. The sand had a mean grain size D_{50} of 0.31 mm and a coefficient of uniformity U_c of 2.0. After setting a pile group in the laminar box, the bottom non-liquefiable layer around the pile group was made with cement-mixing sand and that away from the pile group with air-pluviation and compaction of the sand. The dry sand was also air-pluviated to form the liquefiable layer. The relative densities of the dense and medium dense sand layers were about 90 % and 60 %, respectively.

To minimize the occupation time of the shaking table platform, the above preparation processes were made on the outside of the shaking table platform, and the laminar box including the dry-sand-pile-foundation system was then moved on to the shaking table platform by two gigantic cranes (Photo 2). The dry sand was then saturated on the shaking table platform with water under a vacuum to avoid unexpected soil disturbance during transportation. Photo 3 shows that the laminar box was being covered with a large bell-shaped cover to form a vacuum. The groundwater table was set at a depth of 0.4 m below the ground surface.

Table 1 summarizes the test conditions in the tests where foundations with and without a superstructure were used. Model A carried no superstructure, whereas Model B carried a superstructure of 12 tons with four steel columns of 1.0 m height. About 900 sensors including strain gauges, accelerometers, velocity meters, earth pressure transducers, pore water pressure transducers, displacement transducers, settlement meters and load cells were placed in the sand deposit as well as on the pile-structure model.

The tests were conducted under two-dimensional shaking with two different ground motions recorded at Takatori in the 1995 Kobe earthquake and at Akasaki in the 2000 Tottori earthquake (hereby named Takatori
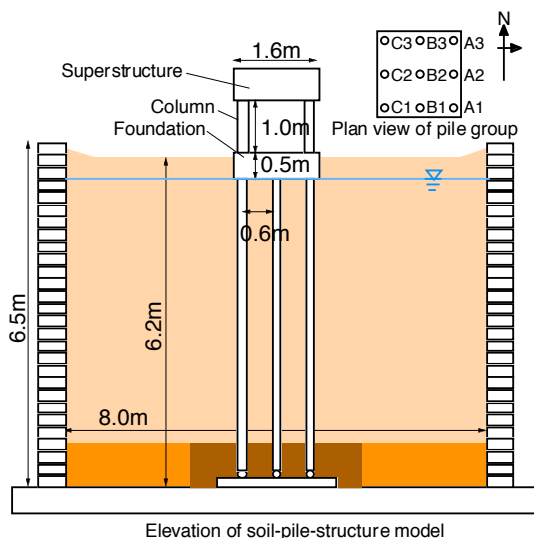
Figure 1 Soil-pile-structure model

Photo 1 Laminar box on shaking table

Photo 2 Laminar box carried by two cranes

Photo 3 Laminar box being covered for saturation

Table 1 Test conditions

Test model	Superstructure	Input motion	Maximum input acceleration
Model A	No	Tottori	0.3 m/s^2, 0.8 m/s^2
		Takatori	0.3 m/s^2, 0.8 m/s^2
Model B	Yes	Tottori	0.3 m/s^2, 0.8 m/s^2
		Takatori	0.3 m/s^2, 0.8 m/s^2, 3.0 m/s^2

and Tottori). Fig. 3 shows the acceleration response spectra of those motions, which were computed from acceleration records, on the assumption that a damping was 5 %. The acceleration response spectra of the horizontal motions at Tottori dominate only in a short period range with a sharp spectral peak at about 0.1 s (Fig. 3(b)), whereas those at Takatori dominate over a wide period range covering from 0.1 s to 1.0 s (Fig. 3(a)). For each test model, two horizontal component motions were used as the input to the shaking table with the largest horizontal acceleration adjusted from 0.3 m/s^2 to 3.0 m/s^2, as shown in Table 1. The NS and EW components of the ground motion were applied to the NS (X) and EW (Y) directions as shown in Fig. 1.

All the pile heads yielded, when Takatori was applied to Model B with a maximum acceleration of about 3.0 m/s^2. As a result, the foundation suffered residual deformations of 66 mm on the east and of 43 mm on the south, accompanied by settlements of 16 mm on the southeast side and of 8 mm on the northwest side. This paper describes inertial and kinematic effects on deformation and failure modes of piles based on the tests in which Tottori and Takatori with maximum input accelerations of 0.8 m/s^2 and 3.0 m/s^2 were applied to Model B. These tests are hereby called as Tottori-80, Takatori-80 and Takatori-300.

3. SOIL-PILE-STRUCTURE INTERACTION IN LIQUEFIABLE GROUND

3.1. Difference in observed major values among three tests

Figs. 4-6 show the NS and EW time histories of bending strains at the head of Pile A1, displacements of the ground surface, and accelerations of the superstructure and the shaking table, together with those of the excess pore water pressures at three depths in the soil for the three tests. The time histories of the pore water pressure, displacement and accelerations are significantly different between Tottori-80 and Takatori-80, regardless of the same level of input acceleration. Namely, the pore water pressure increases slightly, and does not reach the initial effective stress in Tottori-80 (Fig. 4(b)), resulting in a small ground displacement and a superstructure acceleration that is larger than the input acceleration (Fig. 4(c)-(e)). This suggests that the behavior of the pile-

structure system in non-liquefied soil is more or less similar to that in dry sand. The pore water pressure in Takatori-80 with the same maximum input acceleration, in contrast, increases significantly and reaches the initial effective stress (Fig. 5(b)), accompanied by larger ground displacements (Fig. 5(c)). As a result, the superstructure acceleration, which is larger than the input acceleration before pore pressure generation, becomes smaller than the input acceleration after soil liquefaction (Fig. 5(b)(d)(e)). This confirms that the behavior of the pile-structure system becomes completely different from before once soil liquefaction occurs and suggests that not only the occurrence of soil liquefaction but also the soil-pile-structure interaction is significantly affected by the type of input ground motions.

As expected, the bending strain in the pile in the liquefied case (Takatori-80) is larger than that in the non-liquefied case (Tottori-80) (Figs. 4 and 5(a)). In particular, the bending strain in the liquefied case increases significantly after liquefaction but remains within the elastic range. Considering the de-amplification of the superstructure acceleration after liquefaction, an increase in ground displacement in this case could have significant effects on the increase in bending strain.

The pore water pressures in Takatori-300 with the largest input acceleration rises abruptly leading complete liquefaction at only 4 s (Fig. 6(b)). The ground displacement becomes larger and the de-amplification of the superstructure becomes more pronounced than those in Takatori-80 with a smaller input acceleration (Figs. 5 and 6(c)(d)). This could lead to a larger bending strain of about 3000 μ, suggesting the yielding of the pile heads during this test (Fig. 5(a)).

3.2. Distribution of pile stresses within pile group

To investigate distribution of pile stresses within the pile group, Figs. 7 shows the loci on the horizontal plane of the inertial force, the displacements of the ground surface and foundation, and the bending strain at the head of Pile A1. Fig. 8 shows the distributions with depth of bending and axial strains for the nine piles at two instants (i.e., at 2.9 s (before liquefaction) and at 7.9 s (after liquefaction)) in Takatori-80, which correspond to the instances marked by square and circle symbols on the loci shown in Fig. 7.

Figure 2 Grain size distribution
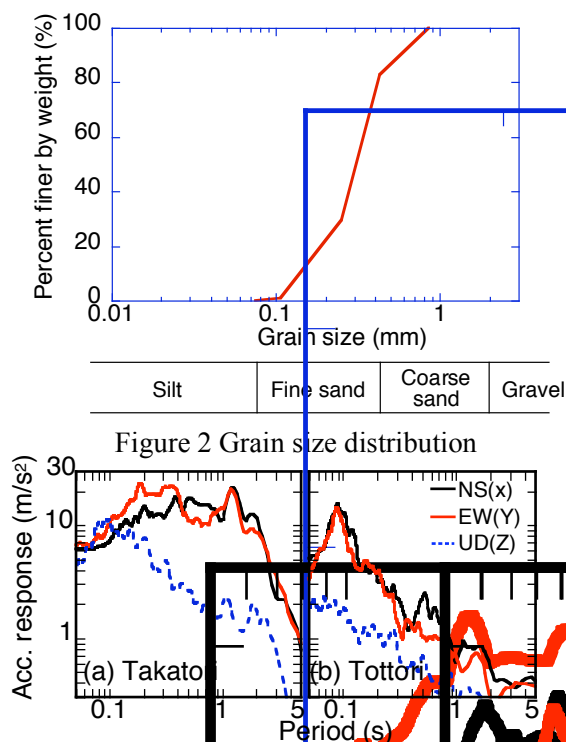
Figure 3 Acceleration response of input motion
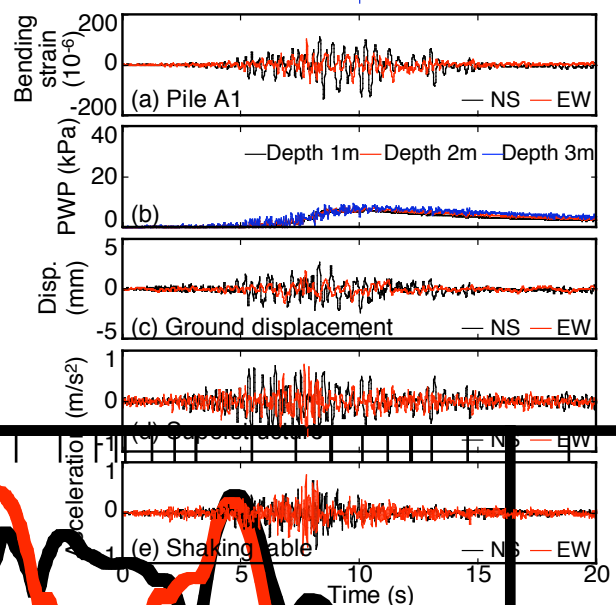
Figure 4 Time histories of major values in Tottori-80

A large inertial force acts eastward at 2.9 s (the square symbol in Fig. 7(a)), accompanied by a very small ground displacement. This not only induces bending strains that decrease rapidly with depth (Fig. 8(a)-(c)) but also creates the largest bending strain at the heads of the leading piles (Piles A1, A2 and A3) probably due to the shadowing effects of pile group, in which the leading piles attract the largest earth pressure among others. In addition, the largest axial compression (negative) strain develops on the leading side of the pile group (Piles A1,
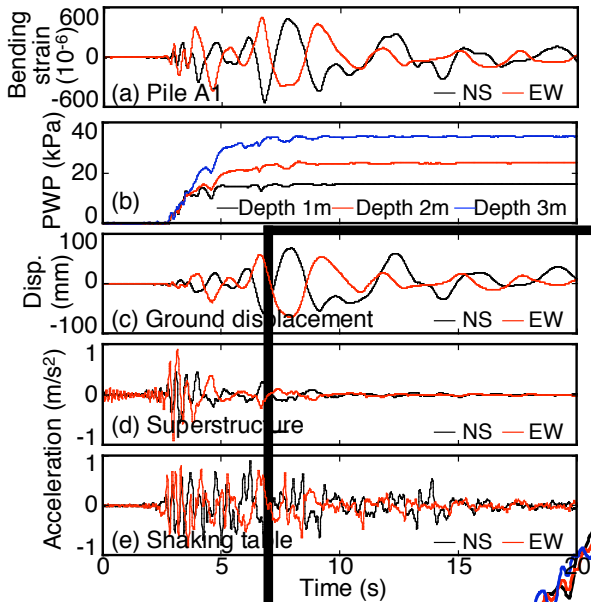
Figure 5 Time histories of major values in Takatori-80   Figure 6 Time histories of major values in Tottori-80
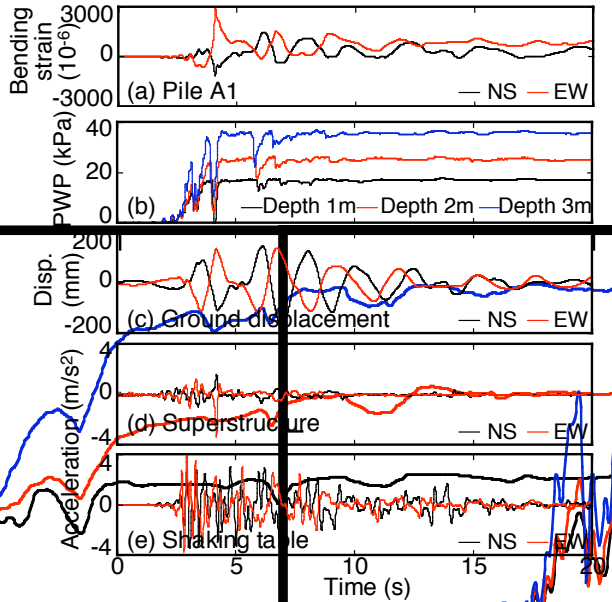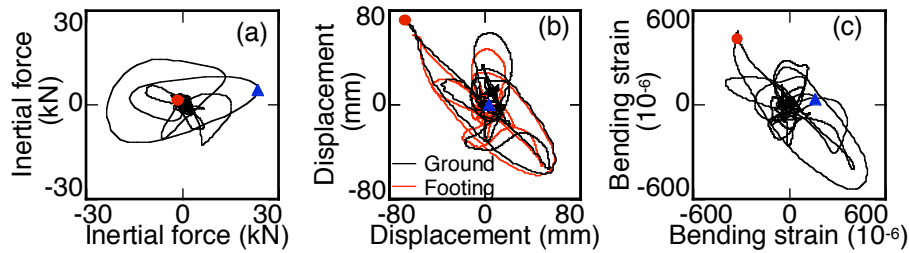
Figure 7 Horizontal loci of inertial force, displacement and bending moment in Takatori-80
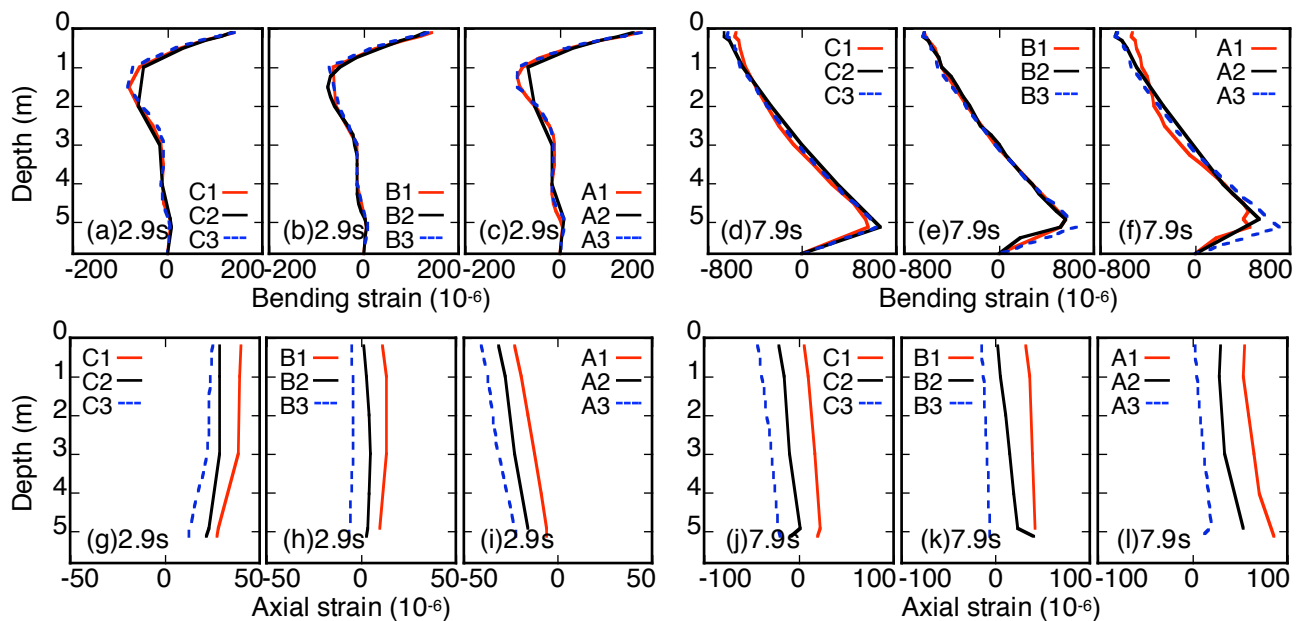
Figure 8 Distribution of bending and axial strains in Takatori-80

A2 and A3), with the largest axial extension (positive) strain on the rear piles (Piles C1, C2 and C3) (Fig. 8(g)-(i)).   The axial strain in this case decreases with depth.   In contrast, a large ground displacement occurs northwestward with a small inertial force at 7.9 s, as indicated with the circle symbol (Fig. 7(a)(b)).   At this moment, large bending strains occur not only at the pile heads but also at the bottom of the liquefied layer.   The bending strain at the pile heads is the smallest in Pile A1 located at the following side (the southeast side) among others (Fig. 8(d)-(f)).   The axial strains on both compression and extension sides do not seem to decrease with depth (Fig. 8(j)-(l)), the trend of which is different from that before liquefaction, and suggests that the positive friction reducing the axial stress in piles becomes smaller due to the occurrence of soil liquefaction.

Fig. 9 shows the relations of excess pore water pressure measured on the pile surface at a depth of 1 m and pile head displacement in the northeast-southwest direction for the three piles (A1, B2 and C3) in Takatori-80.   The pore water pressures used are those observed on the north of the piles in Fig. 9(a)(e)(i) (C3_N, B2_N and A1_N), those on the south in Fig. 9 (d)(h)(l) (C3_S, B2_S and A1_S), those on the east in Fig. 9 (c)(g)(k) (C3_E, B2_E and A1_E), and those on the west in Fig. 9 (b)(f)(j) (C3_W, B2_W and A1_W).   The southwestward displacement is assigned a positive value in Fig. 9.   The pore water pressure after reaching the initial effective stress cyclically decreases with increasing pile displacement.   It is interesting to note that the pore water pressure reduction varies depending on its measurement location.   Namely, when the pile displacement increases southeastward or a positive displacement occurs, the decrease in pore water pressure is the largest on the north and west sides of Pile C3 located on the northwest side (Fig. 9(a)(b)).   In contrast, when the pile displacement increases northwestward or a negative displacement occurs, the decrease in pore water pressure is the largest on the south and east sides of Pile A1 located on the southeast side (Fig. 9(k)(l)).   This suggests that the pore water pressure reduction is significant on the rear side of the following pile.   Because the bending strain at the pile head at 7.9 s is the smallest in the following pile (Pile A1) among others (Fig. 8(d)-(f)), the following pile is probably pulled back due to pore water pressure reduction in the soil on the rear side.   This indicates that the difference in pore water pressure reduction might have affected the difference in bending strain in liquefied ground.

Figs. 10 and 11 show loci of horizontal plane of the inertial force, ground surface and foundation displacements, bending strain at the head of Pile A1 and distributions of bending and axial strains for the nine piles at 4.2 s in Takatori-300.   The ground displacement and the inertial force increase southeastward at 4.2 s as indicated with a circle symbol (Fig. 10), causing large bending strains at the pile heads.   The bending strain at the pile head takes the largest value in the leading piles (Piles A1, A2 and A3), (Fig. 11(a)-(c)).   The axial strain also
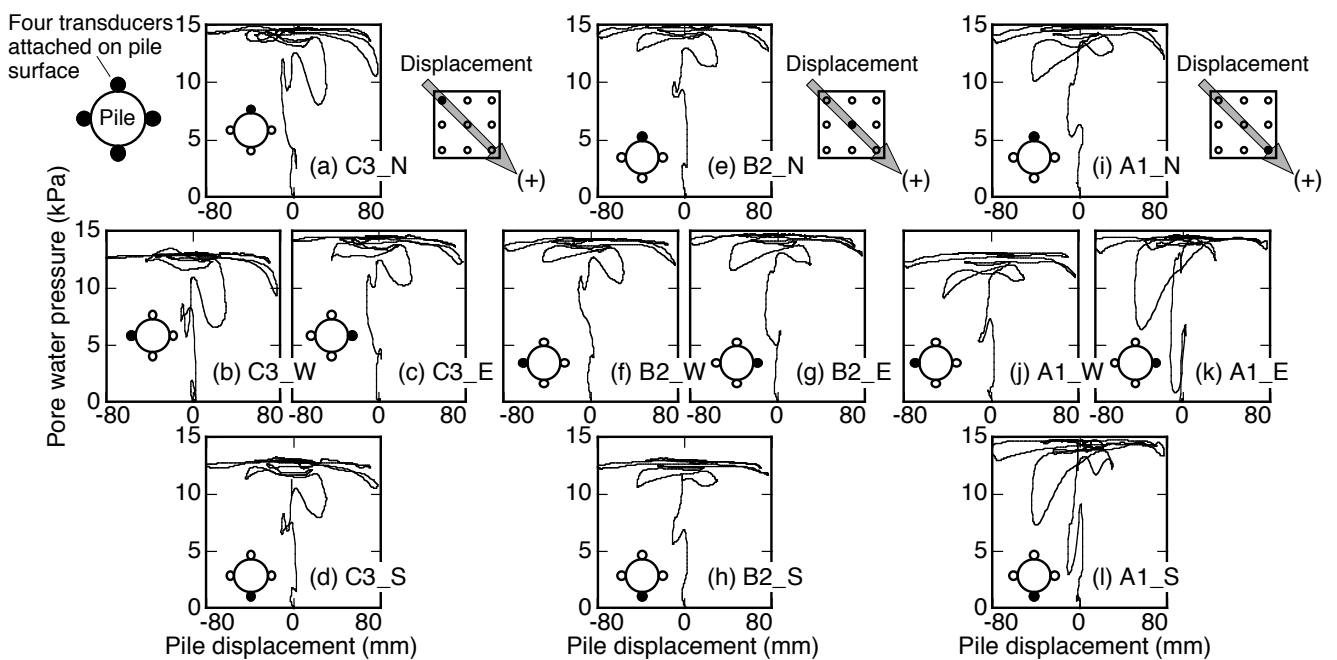
Figure 9 Excess pore water pressure changes in soil around piles in Takatori-80

increases significantly at the pile heads on the leading side (Piles A1, A2 and A3) (Fig. 11(d)-(f)).

Fig. 12 shows the relations of the excess pore water pressure measured on Piles A1, B2 and C3 at a depth of 1.0 m and pile heads displacement in the northeast-southwest direction. When the pile displacement increases southeastward at 4.2 s as indicated in circles, the pore water pressure decrease becomes significant on the north and west sides (rear side) of the following pile (Pile C3) in Fig. 12(a)(b). Considering that the bending strain at 4.2 s is smaller in Pile C3 than others, the pore water pressure decreases might have affected the variation of bending strain within the pile group. In addition, the axial stress varies depending on the location within the pile group, resulting in difference in pile strain within the pile group. The foundation suffered a significant settlement on the southeast side and thus the residual deformation southeastward, the direction of which corresponds to the strong axis of inertial force and ground displacement.
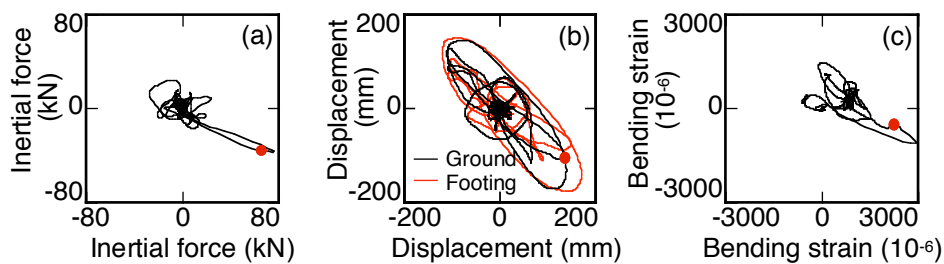
Figure 10 Horizontal loci of inertial force, displacement and bending strain in Takatori-300
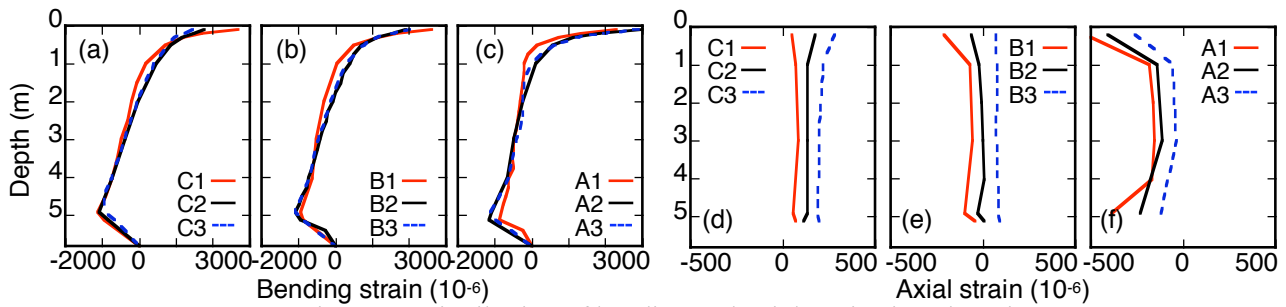
Figure 11 Distribution of bending and axial strains in Takatori-300
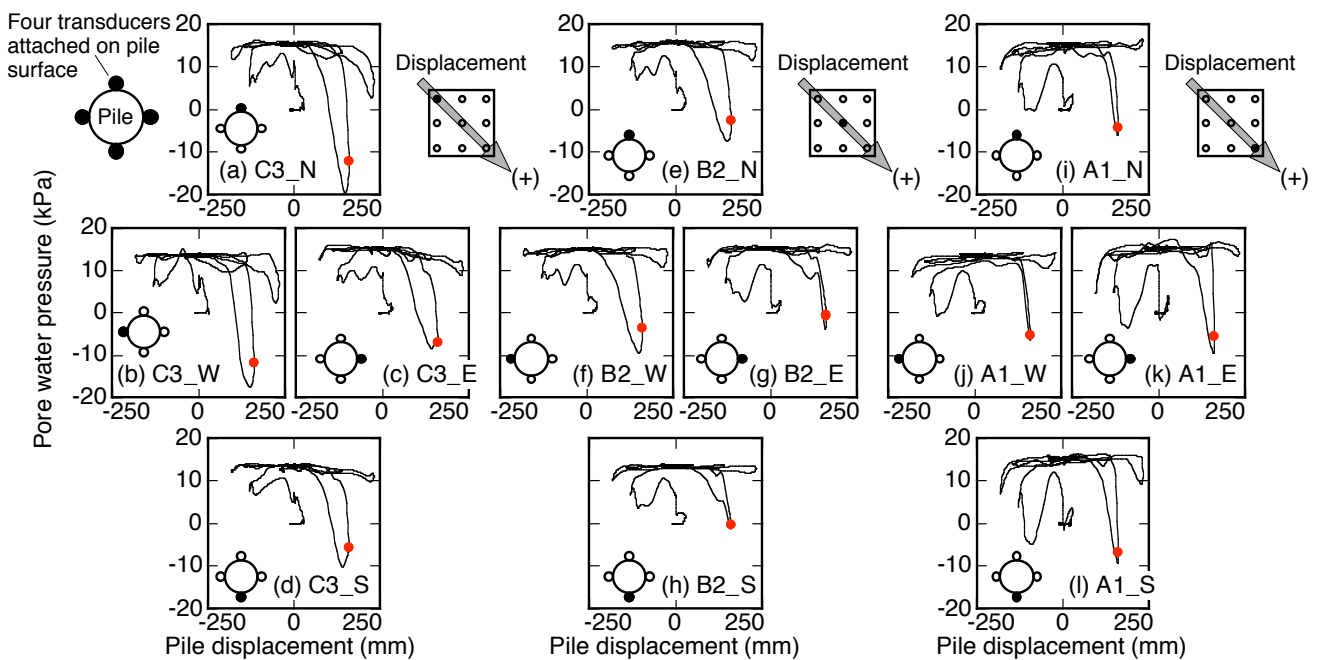
Figure 12 Excess pore water pressure changes in soil around piles in Takatori-300

4. CONCLUSIONS

To investigate soil-pile-structure interaction in liquefied ground, physical model tests were conducted under multi-dimensional loading using the large shaking table at E-Defense, NIED.   The test results and discussions led to the following conclusions:

1) The first geotechnical test on a liquefiable soil-pile-structure model using E-Defense shaking table and two-dimensional laminar box was made without any significant problem.   About 900 sensors installed in the test model were in good conditions throughout the tests and could provide valuable data.   The generation of excess pore water pressures and soil-pile-structure interaction vary significantly depending not only on the maximum acceleration but also on the type (frequency components) of the input motions.

2) The bending strain becomes the largest in the leading pile but the smallest in the following pile.   The difference in bending strain might have been induced by the shadowing effects of pile group in the non-liquefied soil and by the pore water pressure changes in soil around the piles in the liquefied soil.   This indicates that the stress state in soil around piles is completely different between the non-liquefied and liquefied soil.   In addition, the axial strain in piles decreases with depth in non-liquefied ground but is almost constant in liquefied ground, probably due to the reduction in positive frictional resistance of the pile during soil liquefaction.

3) All the pile heads yielded in Takatori-300 with the largest input acceleration, causing residual deformation and settlement of the foundation in the direction of the strong axis of the inertial force and ground displacement.   The damage to piles was significant on the leading side, which might have induced by the difference in bending and axial strains within the pile group.

ACKNOWLEDGEMENTS

REFERENCES

Mizuno, H., Sugimoto, M., Iiba, M., Hirade, T. and Mori, T. (1997). Evaluation of seismic behavior of pile foundations and seismic action on piles by shaking table tests of large-scale shear box (Part 5 Plan and intention of shear box shaking table tests (liquefaction) and soil characteristics), *Proc. of Japan National Conference on Architecture and Building Engineering*, **B-2**, 377-378 (in Japanese).

Tamura, S., Minowa, C., Fujii, S., Yahata, K., Tsuchiya, T., Kagawa, T. and Abe, A. (1998). Shaking table test of reinforced concrete pile foundation on liquefied soil using large scale laminar box (Part 1 Outline of test), *Proc. of Thirty-third Japan National Conference on Geotechnical Engineering*, **1**, 819-820 (in Japanese).

Boulanger, R. W., Curras, J. C., Kuter, B. L., Wilson, D. W. and Abghari, A. (1999). Seismic soil-pile-structure interaction experiments and analyses, *Journal of Geotechnical and Geoenvironmental Engineering,* ASCE, **125:9**, 750-759.

Saito, H., Tanaka, H., Ishida, T., Koyamada, K., Kontani, O. and Miyamoto, Y. (2002). Vibration tests of pile-supported superstructure in liquefiable sand using large-scale blast (Outline of vibration tests and responses of soil-pile-structure), *Journal of Structural and Construction Engineering*, **553**, 41-48 (in Japanese).

Tabata, K. and Sato, M. (2006). Report of special project for earthquake disaster mitigation in urban areas, Ministry of Education, Culture, Sports Science and Technology, 489-554, (in Japanese).

Tabata, K., Sato, M. and Tokuyama, H. (2007). Report of special project for earthquake disaster mitigation in urban areas, Ministry of Education, Culture, Sports Science and Technology: 466-546, (in Japanese).

Tokimatsu, K., Suzuki, H., Tabata, K. and Sato, M. (2007). Three-dimensional shaking table tests on soil-pile-structure models using E-Defense facility, *Proc. of 4th International Conference on Earthquake Geotechnical Engineering*, 11 pp.